Rapid Communications

Clogging-jamming connection in narrow vertical pipes

Diego López, Dariel Hernández-Delfin, Raúl C. Hidalgo, Diego Maza, and Iker Zuriguel*
Departamento de Física, Facultad de Ciencias, Universidad de Navarra, E-31080 Pamplona, Spain

(Received 22 July 2019; revised 9 May 2020; accepted 2 July 2020; published 20 July 2020)

We report experimental evidence of clogging due to the spontaneous development of hanging arches when a granular sample composed of spherical particles flows down a narrow vertical pipe. These arches, akin to the ones responsible for silo clogging, can only be possible due to the role of frictional forces; otherwise they will be unstable. We find that, contrary to the silo case, the probability of clogging in vertical narrow tubes does not decrease monotonically with the ratio of the pipe-to-particle diameters. This behavior is related to the clogging prevention caused by the spontaneous ordering of particles apparent in certain aspect ratios. More importantly, by means of numerical simulations, we discover that the interparticle normal force distributions broaden in systems with higher probability of clogging. This feature, which has been proposed before as a distinctive feature of jamming in sheared granular samples, suggests that clogging and jamming are connected in pipe flow.

DOI: 10.1103/PhysRevE.102.010902

When a system composed of many bodies passes through a constriction, clogging may appear due to the spontaneous formation of local structures that arrest the flow [1–3]. Clogging has been traditionally investigated in bottleneck flows, a phenomenon affecting several many-body systems such as pedestrians [4–7], colloidal suspensions [8,9], active matter [10], or granular media [11–18]. From these works, it is known that the development of clogs is memory independent as the clogging probability is constant for given experimental conditions [11,19–21]. Also, it is well accepted that the ratio outlet-particle size is the most important variable in determining clogging probability: The average flow duration preceding a clog monotonically increases with the outlet size [12–14].

Recently, a clogging phase diagram [22] that resembles the jamming one [23], has been proposed; then arousing an important debate on to what extent the phenomena of clogging and jamming are related. In principle, clogging is triggered by a local structure (the arch) that drives the system to a metastable configuration, whereas a jammed state is characterized by a motionless homogeneous arrangement whose rigidity diverges as the critical density is approached. This is, basically, the main conclusion of a series of works in which disks were driven through obstacles [24–27]. As a result of this interpretation, it turns out that jamming involves the whole system, whereas clogging is primarily related to the bottleneck region.

For these reasons, the passage of an assembly of grains through a narrow pipe seems a good scenario to further investigate this divisive topic. As in this geometry there is not constriction, clogging in pipes implies the formation of a dome spanning the whole system size, at least in one direction [Fig. 1(b)]. Surprisingly, the number of works on this topic is scarce, and a connection between clogging and jamming is missing. In [28], spherical beads were shown to clog when flowing through a narrow channel of very rough walls (sawtooth shaped). Also, clogging was reported for faceted particles (stones) within inclined smooth tubes discharged through a belt at the bottom [29]. Finally, Verbücheln *et al.* [30] numerically showed that a very diluted sample of spheres falling under the force of gravity within an infinitely long vertical narrow tube could clog after forming a dense cluster. Nevertheless, to our knowledge, there is not any experimental evidence of clogging of spheres in smooth vertical tubes.

In order to investigate this problem, we have designed an experimental setup consisting of a vertical narrow pipe full of grains which are extracted at a constant rate by means of a conveyor belt placed at the bottom [Fig. 1(a)]. The pipes are 2 meters long, have an inner diameter D ranging from 10 to 26 mm, and are made of transparent polymethyl methacrylate. This material allows the observation of clogs and was observed to be very stable in combination with Delrin spheres [31]. The latter also have different diameters, d, from 5 to 8 mm, and are used in either monodisperse or bidisperse samples. The grains are extracted by a 60-mm-width conveyor belt placed 10 mm below the pipe and running at $v = 2.2$ mm/s. The system is complemented by ten independent electric shakers that hit the back of the pipe to remove the clogs; a top reservoir from which the grains are poured into the tube; a bottom reservoir that collects the grains; and two cameras (a webcam at the top, and a HD camera on the side).

The measuring protocol is the following: First, the pipe is filled through the reservoir at the top [31]. Then, the conveyor belt is switched on and the material starts flowing down the pipe; this instant is defined as t_{start}. When eventually, a hanging dome clogs the pipe, all the material above it stops. This moment (t_{end}) is detected by means of a real-time image analysis using the top camera with a resolution of 0.1 s. Then, a picture of the entire pipe is taken by the lateral camera and analyzed in order to identify the position of the clog, which is destroyed by activating the nearest shaker above it. Finally, the conveyor belt is switched on, initiating a new measurement until around 500 data points are obtained for each experimental condition.

*iker@unav.es

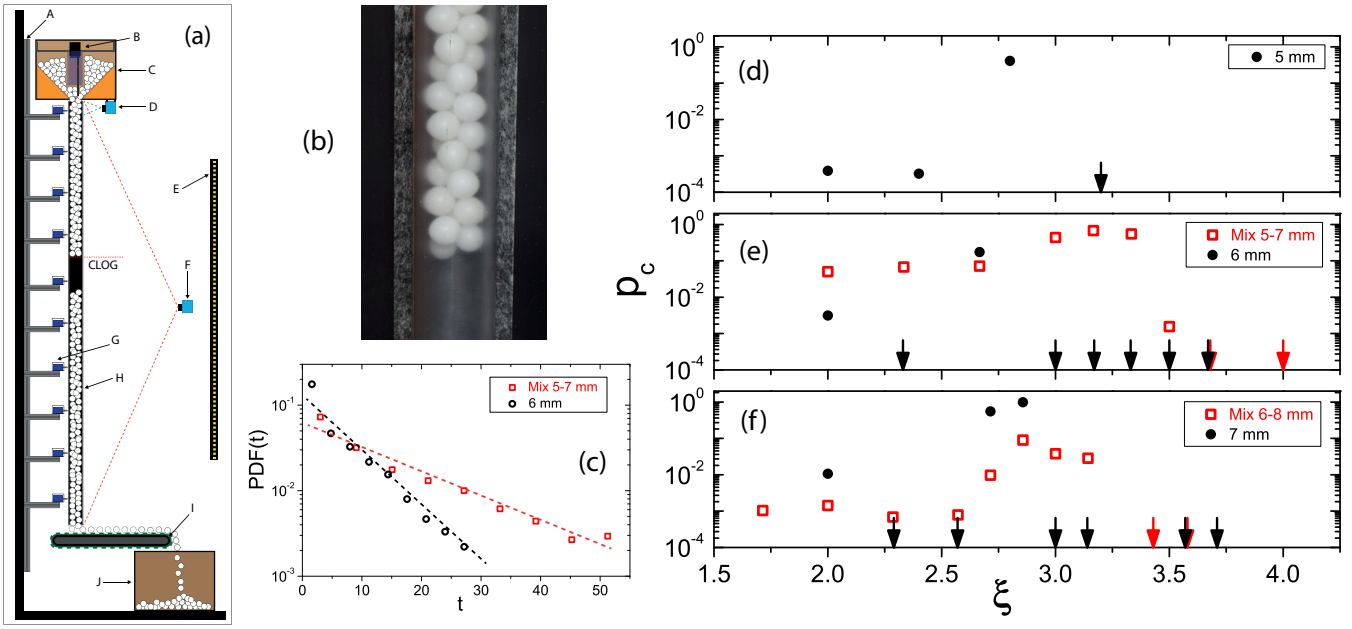

FIG. 1. (a) Sketch of the experimental setup. (A) Aluminum framework attached to the laboratory wall in which ten independent shakers (G) are placed at 20 cm distance. (B) Apparatus devised to fill the vertical pipe (H) from the top reservoir (C). (D) Top and (F) lateral cameras, and (E) LED panel. (I) Belt that extracts the material and deposits it in a bottom reservoir (J). (b) Photograph of a hanging arch. (c) Probability distribution function (PDF) of the flowing intervals t for an aspect ratio of $\xi = 2.67$ when using monodisperse (6 mm) and bidisperse (5 and 7 mm) samples as indicated in the legend. The dashed lines correspond to exponential fittings (note the log-lin scale). The faster decay for the monodisperse case corresponds to a higher value of p_c in panel (e). (d), (e), and (f) show the probability of clog formation versus ξ for monodisperse and bidisperse samples as indicated in the legend. The arrows indicate experiments for which no clogs are observed after more than 4–5 h of flow; hence implying $p_c < 10^{-4}$.

The first meaningful result is that, effectively, the flow of equally sized grains in a smooth vertical pipe can be halted due to the formation of hanging arches. Also, we found that in all the experimental conditions the duration of flowing intervals $t = t_{\text{end}} - t_{\text{start}}$ is distributed exponentially [Fig. 1(c)]; hence suggesting a constant probability of clog formation over the whole discharge process similar to that of bottleneck clogging [11,14,19–21]. It is well known that the probability that the system gets clogged per unit time can be calculated in a straightforward manner as $p_c = (\langle t \rangle) + 1)^{-1}$ [32]. Then, in Figs. 1(d)–1(f), we plot p_c against the pipe diameter rescaled by the sphere diameter ($\xi = D/d$) for several monosized samples. Surprisingly—and contrary to the behavior observed in bottleneck flows—we spot erratic behavior: Clogging is rather likely in the regions where $2.7 < \xi < 3$ and $\xi \sim 2$, whereas it is extremely rare when $2 < \xi < 2.7$ and $\xi > 3$. The absence of clogs for values of $\xi > 3$ can be justified by a low probability of large arches forming. Whereas in bottlenecks this transition occurs for $D/d \approx 5$ [12–14], a shift to lower values is to be expected in straight pipes due to the special nature of the hanging arches causing the clogs. Nevertheless, the absence of clogging for $2 < \xi < 2.7$ and the sudden drop of p_c for $\xi = 3$ are two features that cannot be explained based on the existing knowledge on bottleneck clogging.

As proposed in [30], the absence of clogging for some specific aspect ratios could be related to a spontaneous development of ordering in the packing. Remarkably, the formation of periodic structures within narrow tubes is a topic of great interest in many fields [33–37]. Nevertheless, with some exceptions [33], its study has been mainly conducted from a theoretical or numerical point of view: Following either annealing processes [34,35], sequential deposition protocols [36], or adaptive-shrinking cells [37]. As the spontaneous formation of these structures is favored for monodisperse samples [33], we decided to indirectly test this hypothesis using bidisperse mixtures. We used two different sets of 5 and 7 mm, or 6 and 8 mm spheres (50% in weight) for which an equivalent diameter of $d_{\text{eq}} = 6$ and 7 mm was defined, respectively (see [31] for a precise definition of d_{eq} and its effect in the obtained results). The dependence of p_c on ξ for bidisperse mixtures [Figs. 1(e) and 1(f)] reveals that the range of ξ at which clogs develop is enlarged, extending past $\xi = 3$. Also, we observe flow arrest in the region of $2 < \xi < 2.7$ where the pipe never clogged in the case of monodisperse samples. Nevertheless, a reminiscence of the behavior reported for the monodisperse case is also evident for bidisperse mixtures as p_c does not monotonically decrease with ξ.

Aiming to shed light on this counterintuitive phenomenon, we implemented numerical simulations which can provide information on the three-dimensional structure of the packings and the force transmission within the grains. We used discrete element modeling (DEM) accounting for particle-particle and particle-wall contacts, hence reproducing the dynamics of each particle. We implemented a linear-dashpot model with $k_n = 6.85 \times 10^4$ N/m and $k_t = 2/7k_n$ for the normal and tangential stiffness, respectively. The density of the particles is $\rho = 1360$ kg/m^3 and the coefficient of restitution is $e = 0.9$ for both particle-particle and particle-wall interaction. For the calculations, we used MercuryDPM, which is a well-known DEM simulator [38].

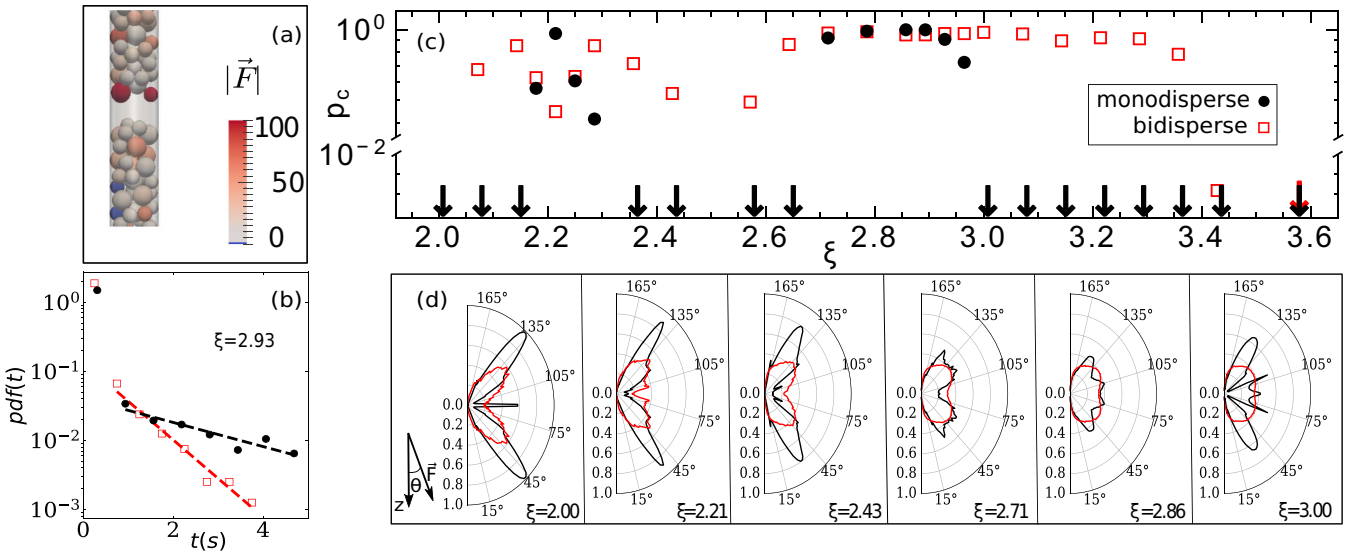

FIG. 2. (a) Illustration of a simulated hanging arch with beads colored depending on the weight they are supporting (rescaled by the weight of a single particle) as shown in the scale. (b) PDF of the flowing intervals duration t when $\xi = 2.93$ for monodisperse and bidisperse samples as indicated in the legend of (c). The dashed lines correspond to exponential fits (note the log-lin scale). The faster decay for the bidisperse case corresponds to a higher value of p_c in panel (c). (c) Probability of clogging versus ξ in semilogarithmic scale for monodisperse and bidisperse samples. Arrows are used to underline the values of ξ for which no clogging is observed in the whole simulated time, implying $p_c < 10^{-4}$. (d) Normalized polar distribution of the angles formed between the contact forces and the gravity direction, for different values of ξ. Black and red lines correspond to the monodisperse and bidisperse cases, respectively.

The simulated system consists of a vertical pipe of diameter D, which is initially filled with $N = 500$ spherical particles of diameter $d = 7$ mm. As in the experiments, we also examined a 50% mass mixture of particles with $d = 6$ and 8 mm ($d_{\text{eq}} = 7$ mm). To mimic the experimental particle extraction procedure, we take the particles at the base (those within a region of height $\Delta_h = 2d$) and we fix their vertical velocity to $v_e = 7$ mm/s. These particles act as a mobile base, so in the absence of friction ($\mu = 0$) the whole granular column would move at that constant velocity. When introducing friction ($\mu = 0.4$), however, the formation of hanging domes can halt the flow. When this happens, an empty region develops below the clog [see Fig. 2(a)], a moment in which the mobile base is stopped and the duration of the event is registered. Finally, the clogging arch is removed and the base starts moving again, this procedure being repeated 500 times in most cases. The protocol followed to break the clogging arch consists of removing the particles that are in a thin layer above the empty region (with height of half a particle); the spheres are then placed in the middle of the empty region with a velocity equivalent to that which they would have if falling freely under the force of gravity. Additionally to the flowing time intervals, numerical simulations allow us to calculate the interaction forces and branch vectors. This is done when the moving base is effectively descending (excluding the times in which it is arrested) in order to allow better comparison among results of all pipe diameters irrespective of whether clogging occurs or not [39].

Starting with the monodisperse case, after checking the exponential nature of the distributions of clogging times [Fig. 2(b)], we calculated the clogging probability for different pipe diameters [Fig. 2(c)]. As in the experimental case, we observed a nonmonotonic trend and found the existence of two clogging regions for aspect ratios $2.7 < \xi < 3$ and $\xi \sim 2.2$. Also, for bidisperse samples, we reproduced the experimental finding that p_c augments and becomes different from zero in the region of $2.4 < \xi < 2.7$, and for ξ slightly above 3.0.

As said before, the reason behind this unexpected behavior can be gathered in the spontaneous formation of ordered structures that prevent clog formation. In this regard, aiming to characterize the ordering, several calculations have been performed. The first one concerns the orientation of forces among particles [Fig. 2(d)]. Remarkably, for the monodisperse case, the polar distributions show very sharp peaks for aspect ratios where there is no clogging ($\xi = 2$, 2.43, and 3) which broaden in areas where clogging is frequent ($\xi = 2.21$, $\xi = 2.71$, and 2.86). In the same way, the outcomes of the bidisperse case reveal an overall broadening of the distributions that is less marked for the cases where clogging probability is smaller.

In order to better quantify the degree of ordering developed within the packings, we have built their phyllotactic diagrams [31] and computed the pair-correlation function $g(r)$, but adapted it with regard to the special geometry of our system (Fig. 3). In fact, this calculation has been divided into two different measurements, which consider either the vertical (z) or the spiral radial ($r\theta$) position of the spheres. Clearly, for the monodisperse case, both parameters display very sharp peaks for $\xi = 2$, 2.43, and 3, confirming the emergence of crystallization suggested before for these aspect ratios. Therefore, we confirm that the spontaneous development of crystallization correlates with a reduction of clogging as demonstrated in [30]; otherwise, the existence of disorder seems to favor force transmission towards the walls, which is a necessary requirement for the formation of stable arches.

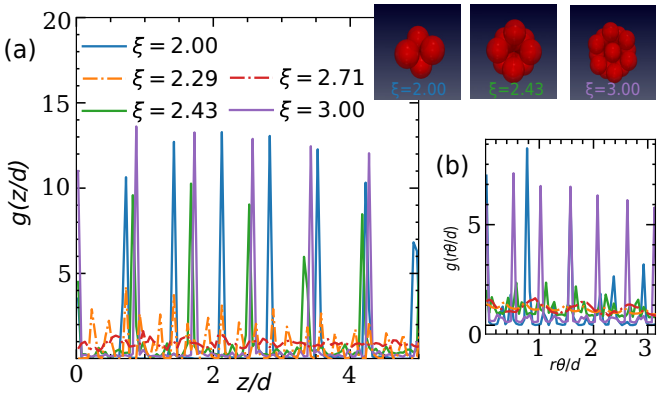

FIG. 3. Pair-correlation function $g(r)$ of monodisperse samples in (a) the vertical (z) and (b) spiral radial ($r\theta$) directions. Bluish and reddish lines correspond to ordered (clogging free) and disordered (clogging prone) packings (see legend for the specific aspect ratios). Top right: Visual representation of the most ordered packings.

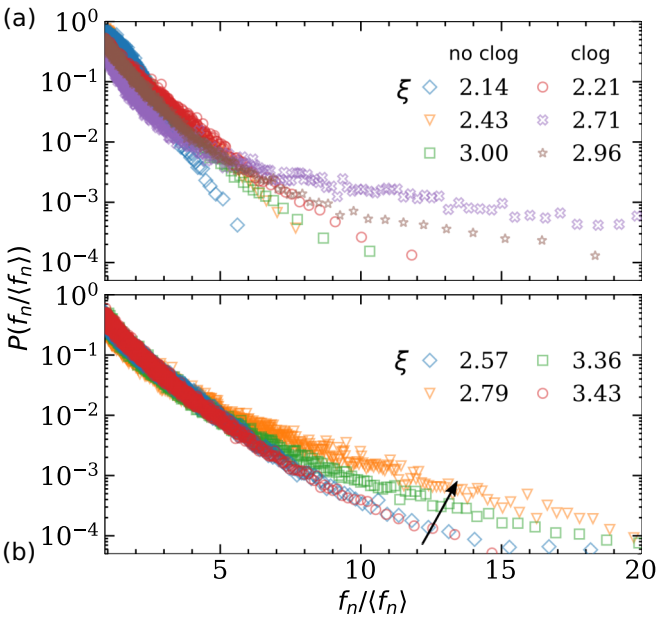

FIG. 4. Normalized distributions of the particle-particle normal forces in (a) the monodisperse, and (b) the bidisperse samples, for several values of ξ as indicated in the legends. In panel (b) the arrow indicates an increase in p_c which correlates with the broadening of the tails.

Finally, in Fig. 4 we show the distributions of the normal forces among particles for several aspect ratios in the monodisperse and bidisperse cases. Remarkably, the distributions display exponential tails that broaden for the scenarios in which clogging is more frequent (i.e., all the bidisperse cases and $\xi = 2.14, 2.43$, and 3 for the monodisperse sample). Even more, in the bidisperse mixture, it is observed that the broader the tail is, the higher the value of p_c [see arrow in Fig. 4(b)]. Interestingly, the broadening of the force distribution tails was already suggested as a distinctive feature of jamming in a sheared system [40]. This analogy may imply that, in our system, clogging is only possible when the ensemble is already close to the jamming transition point. This relationship, which has never been observed in silos, could be caused by the obvious difficulty of getting a clog formed in a pipe (without bottleneck): A clog only appears if the sample is already in a configuration close to jamming. This hypothesis is supported by the fact that, in our experiments, the formation of clogs at several positions at the same time is rather common.

In summary, we have provided experimental confirmation of clogging of spheres in narrow pipes due to the formation of hanging arches. We obtain an exponential distribution of the times that the system is flowing before a clog develops, a feature that can be explained by considering a constant probability of clogging for each experimental condition. Nevertheless, instead of the monotonic decrease of the clogging probability with the outlet size reported in silos, we observe a nonmonotonicity that is attributed to the formation of ordered structures; these prevent the redistribution of forces towards the pipe walls and hence, the stabilization of domes. Finally, we find a notable broadening in the distributions of interparticle normal forces for the scenarios where clogging occurs, suggesting that jamming and clogging could be related in pipe flow. This analogy encourages further research on the flow of grains within this geometry, as it seems especially suitable to throw light upon the extent to which jamming and clogging are connected phenomena.

This work was funded by Ministerio de Economía y Competitividad (Spanish Government) through Projects No. FIS2014-57325 and No. FIS2017-84631-P, MINECO/AEI/FEDER, UE. D.L. and D.H. acknowledge Asociación de Amigos de la Universidad de Navarra for a grant.

[1] D. Helbing, I. J. Farkas, and T. Vicsek, Simulating dynamical features of escape panic, Nature (London) **407**, 487 (2000).
[2] K. To, P. Y. Lai, and H. K. Pak, Jamming of Granular Flow in a Two-Dimensional Hopper, Phys. Rev. Lett. **86**, 71 (2001).
[3] M. D. Haw, Jamming, Two-Fluid Behavior, and Self-Filtration in Concentrated Particulate Suspensions, Phys. Rev. Lett. **92**, 185506 (2004).
[4] S. P. Hoogendoorn and W. Daamen, Pedestrian behavior at bottlenecks, Transp. Sci. **39**, 147 (2005).
[5] T. Ezaki, D. Yanagisawa, and K. Nishinari, Pedestrian flow through multiple bottlenecks, Phys. Rev. E **86**, 026118 (2012).
[6] W. Liao, A. Tordeux, A. Seyfried, M. Chraibi, K. Drzycimski, X. Zheng, and Y. Zhao, Measuring the steady state of pedestrian flow in bottleneck experiments, Phys. A (Amsterdam, Neth.) **461**, 248 (2016).
[7] A. Garcimartín, D. R. Parisi, J. M. Pastor, C. Martín-Gómez, and I. Zuriguel, Flow of pedestrians through narrow doors with different competitiveness, J. Stat. Mech. (2016) 043402.

[8] T. van de Laar, S. ten Klooster, K. Schroën, and J. Sprakel, Transition-state theory predicts clogging at the microscale, Sci. Rep. **6**, 28450 (2016).

[9] A. Marin, H. Lhuissier, M. Rossi, and C. J. Kähler, Clogging in constricted suspension flows, Phys. Rev. E. **97**, 021102(R) (2018).

[10] M. Delarue, J. Hartung, C. Schreck, P. Gniewek, L. Hu, S. Herminghaus, and O. Hallatschek, Self-driven jamming in growing microbial populations, Nat. Phys. **12**, 762 (2016).

[11] I. Zuriguel, L. A. Pugnaloni, A. Garcimartín, and D. Maza, Jamming during the discharge of grains from a silo described as a percolating transition, Phys. Rev. E **68**, 030301(R) (2003).

[12] I. Zuriguel, A. Garcimartín, D. Maza, L. A. Pugnaloni, and J. M. Pastor, Jamming during the discharge of granular matter from a silo, Phys. Rev. E **71**, 051303 (2005).

[13] K. To, Jamming transition in two-dimensional hoppers and silos, Phys. Rev. E **71**, 060301(R) (2005).

[14] C. C. Thomas and D. J. Durian, Fraction of Clogging Configurations Sampled by Granular Hopper Flow, Phys. Rev. Lett. **114**, 178001 (2015).

[15] S. Tewari, M. Dichter, and B. Chakraborty, Signatures of incipient jamming in collisional hopper flows, Soft Matter **9**, 5016 (2013).

[16] A. Ashour, S. Wegner, T. Trittel, T. Börzsönyi, and R. Stannarius, Outflow and clogging of shape-anisotropic grains in hoppers with small apertures, Soft Matter **13**, 402 (2017).

[17] X. Hong, M. Kohne, M. Morrell, H. Wang, and E. R. Weeks, Clogging of soft particles in two-dimensional hoppers, Phys. Rev. E **96**, 062605 (2017).

[18] J. Koivisto and D. J. Durian, Effect of interstitial fluid on the fraction of flow microstates that precede clogging in granular hoppers, Phys. Rev. E **95**, 032904 (2017).

[19] D. Helbing, A. Johansson, J. Mathiesen, M. H. Jensen, and A. Hansen, Analytical Approach to Continuous and Intermittent Bottleneck Flows, Phys. Rev. Lett. **97**, 168001 (2006).

[20] N. Roussel, Thi Lien Huong Nguyen, and P. Coussot, General Probabilistic Approach to the Filtration Process, Phys. Rev. Lett. **98**, 114502 (2007).

[21] T. Masuda, K. Nishinari, and A. Schadschneider, Critical Bottleneck Size for Jamless Particle Flows in Two Dimensions, Phys. Rev. Lett. **112**, 138701 (2014).

[22] I. Zuriguel *et al.*, Clogging transition of many-particle systems flowing through bottlenecks, Sci. Rep. **4**, 7324 (2014).

[23] A. J. Liu and S. R. Nagel, Nonlinear dynamics: Jamming is not just cool any more, Nature (London) **396**, 21 (1998).

[24] H. T. Nguyen, C. Reichhardt, and C. J. O. Reichhardt, Clogging and jamming transitions in periodic obstacle arrays, Phys. Rev. E **95**, 030902(R) (2017).

[25] C. Reichhardt and C. J. O. Reichhardt, Controlled Fluidization, Mobility, and Clogging in Obstacle Arrays Using Periodic Perturbations, Phys. Rev. Lett **121**, 068001 (2018).

[26] H. Péter, A. Libál, C. Reichhardt, and C. J. O. Reichhardt, Crossover from jamming to clogging behaviours in heterogeneous environments, Sci. Rep. **8**, 10252 (2018).

[27] R. L. Stoop and P. Tierno, Clogging and jamming of colloidal monolayers driven across disordered landscapes, Commun. Phys. **1**, 68 (2018).

[28] J.-C. Tsai, W. Losert, G. A. Voth, and J. P. Gollub, Two-dimensional granular Poiseuille flow on an incline: Multiple dynamical regimes, Phys. Rev. E **65**, 011306 (2001).

[29] A. Janda, I. Zuriguel, A. Garcimartín, and D. Maza, Clogging of granular materials in narrow vertical pipes discharged at constant velocity, Granular Matter **17**, 545 (2015).

[30] F. Verbücheln, E. Parteli, and T. Pöschel, Helical inner-wall texture prevents jamming in granular pipe flows, Soft Matter **11**, 4295 (2015).

[31] See Supplemental Material at http://link.aps.org/supplemental/10.1103/PhysRevE.102.010902 for a more detailed explanation of the experimental setup and procedures, as well as an extended description of the particles arrangements observed within the pipe.

[32] D. Gella, I. Zuriguel, and D. Maza, Decoupling Geometrical and Kinematic Contributions to the Silo Clogging Process, Phys. Rev. Lett **121**, 138001 (2018).

[33] A. J. Meagher, F. García-Moreno, J. Banhart, A. Mughal, and S. Hutzler, An experimental study of columnar crystals using monodisperse microbubbles, Colloids Surf., A **473**, 55 (2015).

[34] G. T. Pickett, M. Gross, and H. Okuyama, Spontaneous Chirality in Simple Systems, Phys. Rev. Lett. **85**, 3652 (2000).

[35] A. Mughal, H. K. Chan, D. Weaire, and S. Hutzler, Dense packings of spheres in cylinders: Simulations, Phys. Rev. E **85**, 051305 (2012).

[36] H.-K. Chan, Densest columnar structures of hard spheres from sequential deposition, Phys. Rev. E **84**, 050302(R) (2011).

[37] L. Fu, W. Steinhardt, H. Zhao, J. E. S. Socolar, and P. Charbonneau, Hard sphere packings within cylinders, Soft Matter **12**, 2505 (2016).

[38] T. Weinhart *et al.*, Fast, flexible particle simulations—An introduction to Mercury DPM, Comput. Phys. Commun. **249**, 107129 (2020).

[39] In the scenarios where the system clogs, we have checked that the interaction forces when the system is arrested are similar to when it flows.

[40] E. I. Corwin, H. M. Jaeger, and S. R. Nagel, Structural signature of jamming in granular media, Nature (London) **435**, 1075 (2005).